



Timmons, T., Beeley, J., Bailet, G. and McInnes, C.R. (2022) Experimental Testing of Range-based Relative Positioning Strategies for a Swarm of Centimetre-scale Femto-spacecraft. In: 73rd International Astronautical Congress (IAC), Paris, France, 18-22 Sept 2022.

This is the Author Accepted Manuscript.

There may be differences between this version and the published version. You are advised to consult the publisher's version if you wish to cite from it.

<http://eprints.gla.ac.uk/278368/>

Deposited on: 02 September 2022

Enlighten – Research publications by members of the University of Glasgow
<http://eprints.gla.ac.uk>

IAC-22-B4.IP (68691)

EXPERIMENTAL TESTING OF RANGE-BASED RELATIVE POSITIONING STRATEGIES FOR A SWARM OF CENTIMETRE-SCALE FEMTO-SPACECRAFT

Thomas Timmons, James Beeley, Gilles Bailet and Colin R McInnes

Space and Exploration Technology Group, James Watt School of Engineering, University of Glasgow, Scotland, United Kingdom. G12 8QQ. *t.timmons.1@research.gla.ac.uk

Ongoing miniaturisation within consumer technology now makes it possible to fabricate active femto-spacecraft (mass under 100 g) with inertial measurement units (IMUs), attitude determination and control, radio communications and a suite of sensors packaged on a centimetre-scale printed circuit board. The extension of femto-spacecraft technology to a networked swarm dispersed from a carrier platform could facilitate massively parallel distributed multi-point sensing. Applications include improved investigation of planetary atmospheres, space weather monitoring, magnetospheric characterisation, gravity field mapping and distributed sparse aperture interferometry. For such applications, in-orbit relative navigation would be a key enabling technology. Determining the location of femto-spacecraft relative to one another within a large network would be essential in adding value to data collected, and in enabling femto-spacecraft to operate in proximity to one another; for example, by using differential air drag to maintain the swarm spatial structure. In this paper, we present the results of an experimental test campaign to implement range-based positioning algorithms for a femto-spacecraft swarm, using only coarse estimates of inter-spacecraft range approximated by received signal strength indications (RSSI). This builds on prior work developing and simulating algorithmic approaches using combinations of optimisation and trilateration-based methods to achieve relative positioning with coarse range estimates. A series of experiments and procedures are detailed for the implementation of relative positioning. The development of a suitable path loss model required to use RSSI as a range approximation is detailed, along with real-time networking and localisation techniques.

Nomenclature

c	linear coefficient	API	application programming interface
G	antenna gain	CCS	code composer studio
I	identity matrix	FSPL	free space path loss
N	number of range estimates	GPS	Global Positioning System
n	number of femto-spacecraft	IMU	inertial measurement unit
P	power	I2C	inter-integrated circuit
Rx	receive	LEO	low Earth orbit
r	range	LMI	linear matrix inequality
\hat{r}	range estimate	MEMS	micro-electro-mechanical systems
r_0	reference range	MCU	microcontroller unit
T	period	NLLS	non-linear least squares
Tx	transmit	NPDF	normal probability density function
t	time	PCB	printed circuit board
X	matrix of n femto-spacecraft positions	PLM	path loss model
Z	symmetric positive semidefinite matrix	RSSI	received signal strength indication
α	ranging error	SDK	software development kit
γ	path loss exponent	SDP	semi-definite programming
λ	wavelength	SMA	sub-miniature version A
μ	mean	TI	Texas Instruments
σ	standard deviation	WSN	wireless sensor network
χ	zero mean normal random variable		

1. Introduction

When combined to form a networked swarm, femto-spacecraft could offer many benefits over single small spacecraft for similar applications [1, 2, 3]. Clear functional advantages exist to perform modular and dis-aggregated operations, mitigating component failure concerns. Previous analysis has demonstrated the sensing trade-offs between the traditional use of fewer, larger and more expensive satellites compared with utilising far more femto-spacecraft dispersed from a larger carrier platform [4]. When spatially distributed sensor data is fused to map scalar and vector fields, using a larger number of low-quality measurements can compensate for inaccuracies.

In this paper, we address how a networked swarm of femto-spacecraft could localise relative to one another, without using specific sensors or technology typically required for localisation. The motivation for this approach comes from trying to extract as much functionality from femto-spacecraft swarms as possible, using the benefits of fusing swarm data together. Ranging information can be inferred from network data in the form of the received signal strength indication (RSSI) between two radios. RSSI is a relative index that chipset manufacturers can set their own relative scales for, and is primarily used as an indication of signal quality within a network. In principle, the Friis transmission formula [5] explains the theoretical logarithmic relationship between received radio power and range, but in practice this is not a particularly accurate metric, subject to interference and other wave propagation issues. However, by developing a path loss model with known confidence bounds, and fusing the many RSSIs between an interconnected swarm, relative localisation can be achieved.

In previous work, we have presented algorithmic methods for range-based relative navigation of centimetre-scale femto-spacecraft swarms [6]. The simulation-based results of this work demonstrated range-only relative navigation in both centralised and distributed swarm network configurations. Experimental demonstration of relative positioning is necessary to show practical viability, to determine performance limitations and gain experimental insights. While our previous work assumes the presence of a suitable metric for range, in this paper we address the practical limitations of using RSSI data and the steps taken to convert this into a suitable ranging metric.

The rest of this paper is organised as follows. Section 2 outlines the experimental testing methodology. This covers the development of a swarm network pro-

ocol, path loss modelling to develop a ranging metric, and the methods for experimental testing of relative positioning. Section 3 provides the results and discussion. Conclusions are given in Section 4 .

2. Methodology

This section details our experimental testing methodology. This involves the development of a radio packet network protocol to enable swarm communications suitable for this application, as detailed in Section 2.1, along with extensive outdoor testing of communications. Outdoor experimental testing firstly involved the development of a ranging metric from RF communications, as detailed in Section 2.2, and then the demonstration of range-based relative positioning, as described in Section 2.3. The experimental testing was conducted over several months throughout 2022 on sports pitches at the University of Glasgow’s Garscube Sports Complex.

2.1 Swarm Network Protocol

A network protocol is required for a fully interconnected network of femto-spacecraft. In this section, the development and implementation of this protocol through embedded programming and testing on hardware is detailed.

Texas Instruments (TI) SimpleLink™ sub-1 GHz CC1310 wireless microcontroller (MCU) LaunchPad™ development kits are used as proxies for femto-spacecraft hardware for experimental testing (Fig. 1) [7].

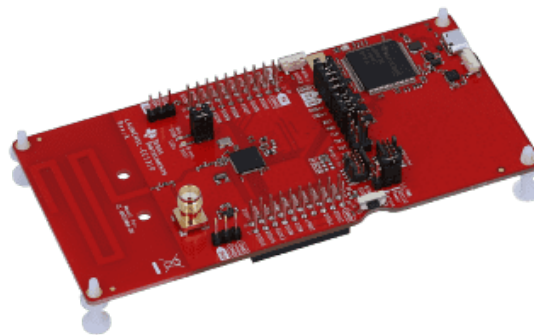


Fig. 1: The TI CC1310 development kit

This development kit is used because its MCU is representative of femto-spacecraft technology in terms of computing power available at the femto-spacecraft mass and length scale, and has an integrated radio module for wireless communications. The development kit has an integrated printed circuit

board (PCB) trace antenna, but also a sub-miniature version A (SMA) port for connecting external antennas. For this experiment, quarter-wavelength 868 MHz V-dipole antennas were fabricated with an SMA port and 0.5 mm diameter copper wire, as shown in Fig. 2. This antenna is chosen as it has an undirected radiation pattern, providing benefits for omnidirectional communications over the integrated PCB trace antenna, as discussed in Section 2.2. The angle between the antenna wires was kept approximately at 90° during testing.

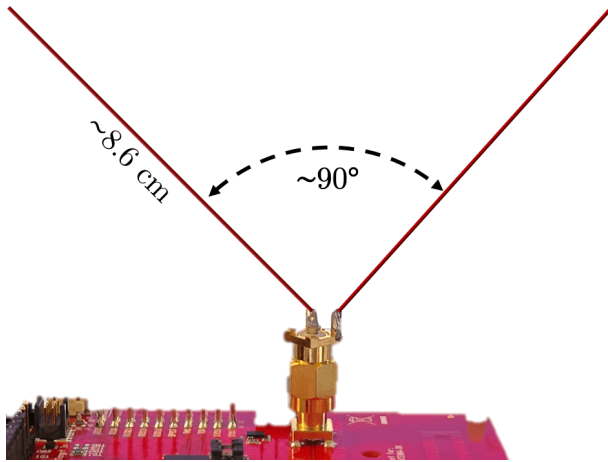


Fig. 2: Quarter-wavelength 868 MHz v-dipole antenna attached to the development kit

The TI EasyLink™ application programming interface (API) is used to develop a custom network protocol. The CC1310 radio module supports half-duplex communications, meaning that development kits can both receive and transmit radio packets, but not simultaneously. This necessitates the development of a protocol that enables full interconnection in a network of multiple femto-spacecraft in any direction as required. Here, we consider full interconnection to be where any femto-spacecraft can both receive from and transmit to any other femto-spacecraft in the network.

For a fully interconnected network of n femto-spacecraft, n transmissions are sufficient to provide all femto-spacecraft with communicated data between all possible $\frac{n(n-1)}{2}$ communication links. Alternatively, $(n-1)$ transmissions are sufficient to provide this data to one femto-spacecraft within the network. This is possible if each femto-spacecraft sequentially transmits while the other $(n-1)$ femto-spacecraft receive and store incoming data. Only RSSI data is of interest in this experiment, but this process would

be essential for sharing sensor and IMU data between femto-spacecraft in practice, and the protocol developed here can easily be modified to accommodate further data flow. This process works by having each femto-spacecraft remain in a receive state until it is their turn to transmit. This is achieved using an address filtering technique, whereby each femto-spacecraft transmits using a different address, making it possible for each femto-spacecraft to be uniquely identifiable to others in the network.

For this experimental demonstration, we only consider a centralised network configuration, as this method has only been tested with up to 14 development kits. It is expected that the approach detailed below would be compatible with a substantially larger number of development kits, however since computational and storage limits would be reached as the number of devices within the network increases, it would be necessary to develop decentralised and distributed network structures and protocols for larger networks. The approach outlined below could be straightforwardly decentralised by having the central femto-spacecraft of one cluster share data with the central femto-spacecraft of another cluster.

As shown in Fig. 3, femto-spacecraft 1 starts the communication sequence by transmitting a radio packet with an empty payload (...) to all other $(n-1)$ femto-spacecraft in the network. As this packet is received, it generates $RSSI_{12}, RSSI_{13}, \dots, RSSI_{1N}$ for those femto-spacecraft to store, respectively, where $RSSI_{ij}$ denotes the received signal strength indication received at femto-spacecraft j from femto-spacecraft i . Then, femto-spacecraft 2 is able to transmit a radio packet containing $RSSI_{12}$ over the network. Then, femto-spacecraft 3 transmits $RSSI_{12,13,23}$, and so on, until femto-spacecraft n has all $\frac{n(n-1)}{2}$ RSSI values between all n femto-spacecraft in the network.

As implemented, when femto-spacecraft 1 transmits, it sets a timer of nT_{delay} before transmitting again, where T_{delay} is a delay period. When femto-spacecraft 2 receives a packet from femto-spacecraft 1, it waits T_{delay} before transmitting. Femto-spacecraft 3 repeats this process upon receiving from femto-spacecraft 2, and so on. This timing sequence can be modified by changing the delay period, where $T_{delay} = 100$ ms in our testing. In this testing, development kit 1 is connected via USB to a laptop, storing and processing incoming data transmitted from development kit n . Development kits $(2-n)$ operate wirelessly and are powered by USB battery packs. In this setup, the laptop can be

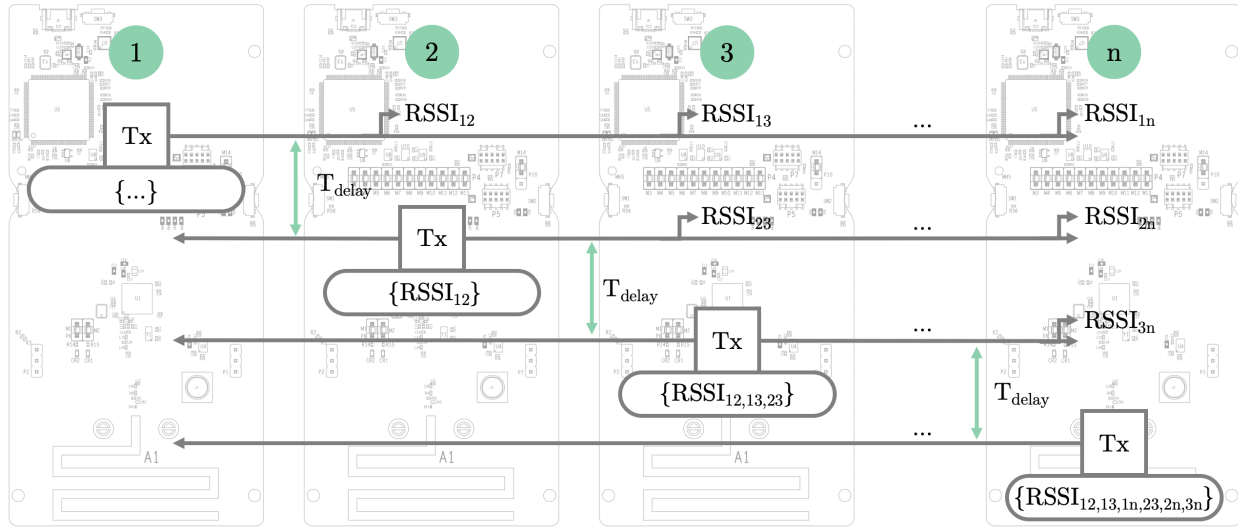


Fig. 3: Wireless data flow in the RSSI gathering protocol

thought of as the central mothercraft for the other femto-spacecraft, which in space could be a CubeSat that deploys the femto-spacecraft swarm.

There are several points to note about this implementation. For simplicity, it is assumed that communication links are undirected (i.e. that $RSSI_{12} \equiv RSSI_{21}$). Otherwise, the number of communication links required would be doubled. In further testing, directed communications could be used to check and reject new RSSI data for the positioning calculations, but this is not considered here (such as in the case where a recent $RSSI_{12}$ measurement is vastly different to a recent $RSSI_{21}$). Secondly, using RSSI data in this way, each femto-spacecraft must transmit at the same power (or at a minimum, transmit at a power known to every other femto-spacecraft), so that the fraction of that power that is received by each femto-spacecraft is properly correlated to range.

The above process flow is realised in software and hardware using the Easylink™ API and building upon TI’s ‘rfEasyLinkEcho’ project [8], which we modify to accommodate the network protocol with address filtering and pre-programmed delay periods. This is developed in C using code composer studio (CCS). The original project demonstrates bi-directional communication between 2 development kits by having one transmit a packet, and another re-transmit (or ‘echo’) that same packet back. We have made substantial modifications to this project to enable full interconnectivity between a network of n development kits within a given time interval. Specifically, we give each development kit a unique transmission address,

and then add an address checking procedure, enabling each development kit to know what data to store and when to transmit. This relies on each node being identifiable by its transmitting address, which is not a limitation, but for dynamically adding nodes to larger networks would likely require a process of identification and synchronisation throughout the network to add nodes that follow this protocol in an ad-hoc fashion. This could be programmed in as an identification process.

Table 1 shows the transmit and receive address structure as implemented. Note that these addresses are given in hexadecimal. Each femto-spacecraft has its own unique transmit address, and a list of addresses that it can receive from (by being pre-set to perform an action once hearing from that specific femto-spacecraft). Note that every femto-spacecraft could be set to use received data from any other femto-spacecraft on the network. For the purposes of this testing and with the assumption of undirected communications, each femto-spacecraft only utilises received data from preceding femto-spacecraft in the network to retrieve relevant RSSI data.

Table 2 shows the radio packet payload structure that all femto-spacecraft use when transmitting. This is used both for allocating incoming RSSI data sequentially, and re-transmitting data to other femto-spacecraft. This shows the payload element array index, the payload contained in that element, and the femto-spacecraft that writes and transmits this data. For brevity, the structure for a 5 node network is shown. The number of payload elements is the same

Table 1: Address filtering structure for the network

Femto-spacecraft	Tx address	Rx address table
1	0x01	0xFF
2	0x02	0x01
3	0x03	0x01,02
4	0x04	0x01,02,03
⋮	⋮	⋮
255	0xFF	0x01,02,03,...,FE

as the number of communication links, $\frac{n(n-1)}{2}$. The radio packet is initially empty, but the appropriate element is filled as each femto-spacecraft transmits in sequence.

Table 2: Radio packet payload structure

Payload element	Payload	Written by
1	$RSSI_{12}$	2
2	$RSSI_{13}$	3
3	$RSSI_{14}$	4
4	$RSSI_{15}$	5
5	$RSSI_{23}$	3
6	$RSSI_{24}$	4
7	$RSSI_{25}$	5
8	$RSSI_{34}$	4
9	$RSSI_{35}$	5
10	$RSSI_{45}$	5

We now outline all modifications to the TI ‘rfEasyLinkEcho’ project in order to realise the network protocol as described above. In the original project showing bi-directional communication between 2 development kits, one development kit runs the ‘rfEasyLinkEchoTx’ program while the other runs the ‘rfEasyLinkEchoRx’ program. The former initialises in a transmit state, transmitting a radio packet every second, switches to a receive state, awaits reception of the echoed radio packet, and if successful, repeats this process continuously. The latter initialises in a receive state, switches to a transmit state upon reception of a radio packet, and after a 100 ms delay, echoes back the received radio packet.

For the fully interconnected network, development kit 1 runs a modified ‘rfEasyLinkEchoTx’ program while all other $(n - 1)$ development kits run different modified ‘rfEasyLinkEchoRx’ programs. Random packet payloads are removed and replaced with a payload structure that is common to all nodes as outlined in Table 2. This payload is represented by an array of

signed integers structured to store RSSI data. RSSI values are stored in the development kit’s internal memory as hexadecimal values, that when converted to decimal, form a signed 2’s complement format corresponding to RSSI in decibel milli-Watts (dBm).

The packet checking task on the ‘rfEasyLinkEchoTx’ program Tx is also removed. In the original project, any received packet must be the same (echoed back). This is no longer the case as the payload is filled by all the development kits in the network. The default packet payload length is increased to accommodate all RSSI data for a given network size.

The delay period (T_{delay}) and transmit wait times are modified to accommodate more than 2 development kits. This is configurable for the desired refresh rate for a given network size, but the basis for our modification is that development kit 1 must repeat transmission at a rate that provides all other development kits with an opportunity to transmit before development kit 1 transmits again. A lower limit on refresh rate has not been tested, and so far testing has successfully shown that a 100 ms delay period between each development kit transmitting works with at least 14 development kits. As described above, development kit 1 waits nT_{delay} (1.4 s for a 14 node network) before restarting the data gathering sequence. As such, the wait time increases as the number of development kits on the networks increases.

Address filtering is added to each program. Development kits store received data in their memory and when it is their turn to, transmit all available data using the common packet payload structure. By default, all development kits except for development kit 1 initialise and default to a receive state. This is only changed upon reception of a packet from a specific development kit. This ensures sequential noiseless transmission. For example, if development kit 3 receives from development kit 1, it will store $RSSI_{13}$ and remain in a receive state. If development kits 3 receives from development kit 2, it will store $RSSI_{23}$ and transmit $RSSI_{13}$ and $RSSI_{23}$.

Development kit 1 communicates received data to a laptop via a serial link. MATLAB is used to read in this serial data live from this program and process it in real time for relative positioning testing. This involves transforming RSSI data into a range estimate by passing it through a path loss model function, then importing it to the relative localisation algorithm. Future work will implement this process in real time onto femto-spacecraft. For this demonstration, computation is handled on a laptop.

2.2 Path Loss Modelling

This section describes the development of a ranging metric from RF communication. For outdoor terrestrial testing, this metric is obtained by developing a path loss model (PLM) for the outdoor environment to test the relative positioning.

In principle, an isotropic transmitter will propagate radio waves equally in all directions of 3-D space. As the wave-front extends outwards from the source, it takes the form of a sphere of ever-increasing size, causing attenuation of the signal's strength in free space according to the inverse-square law. In reality, no antenna is fully isotropic, and undirected (or 'omni-directional') antennas exhibit some degree of directed losses due to antenna wire nulls. Directivity, as a function of angular displacement, is a measure of how directed an antenna's signal is with respect to an ideal isotropic antenna (a directivity of 1, or 0 decibels (dB), refers to isotropic radiation). This parameter, multiplied by an antenna's efficiency (a measure of how well the power supplied to an antenna is radiated), forms the antenna gain. The Friis transmission formula [5], expressed in terms of the gains of the receiving and transmitting antennas, outlines the free space path loss (FSPL) relationship with distance:

$$\frac{P_{Rx}}{P_{Tx}} = G_{Rx}G_{Tx} \left(\frac{\lambda}{4\pi r} \right)^2 \quad (1)$$

where P_{Rx} is the received power, P_{Tx} is the transmitted power, G_{Rx} and G_{Tx} are the receiver and transmitter antenna gains, λ is the signal wavelength and r is the range between the receiver and transmitter.

RSSI relates to the Friis law as the fraction of the received power to the transmit power. As long as the transmit power is constant between multiple femto-spacecraft, network RSSI data will indicate the relative received power. In free space, and with an ideal isotropic radiator, an RSSI value obtained at a receiver positioned anywhere away from the transmitter in 3-D space straightforwardly extends into a precise spherical range relationship between the transmitter and the receiver. In reality, the RSSI value depends upon: free space path loss (theoretically expected signal attenuation); antenna orientation due to anisotropy in propagation; and environmental factors such as the ground, atmosphere, objects and random noise causing reflection, refraction, diffraction and other interference.

From Eq. 1, a logarithmic PLM function can be derived experimentally to account for these effects, taking the form of:

$$PL(r) = PL(r_0) + 10\gamma \log_{10} \frac{r}{r_0} + \chi \quad (2)$$

where $PL(r)$ is the path loss at a path length (range) r away from the transmitter, $PL(r_0)$ is the path loss at a reference range r_0 , γ is the path loss exponent (theoretically 2 for free space, experimentally determined in a given environment) and χ is a zero mean normal random variable.

This PLM function can be developed from experimentation to characterise signal strength decay with range in a given testing environment. This is possible by collecting RSSI data between two radios placed at a series of known ranges away from one another. Once this has been performed, it is possible to refer to this function (and its confidence bounds) and convert RSSI into a range estimate.

In this experimental testing, a PLM is obtained with one-to-one communications between two development kits. Testing in this paper is limited to two dimensional space. As v-dipole antennas are used, their toroidal radiation is expected to largely be isotropic in a 2-D plane, as shown by the model in Fig. 4.

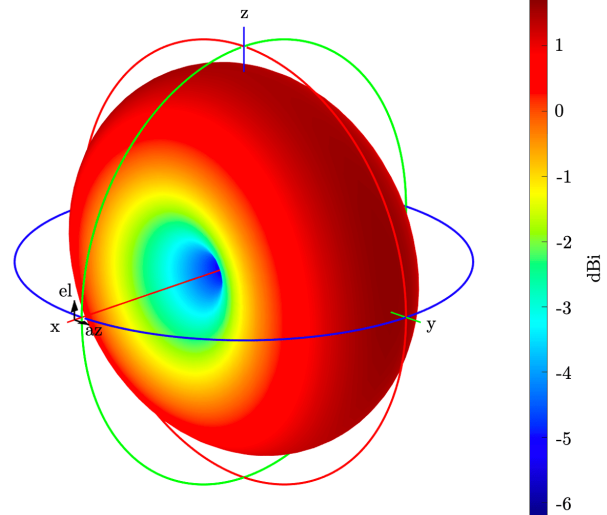


Fig. 4: Theoretical radiation pattern of a quarter-wavelength 868 MHz v-dipole antenna

To develop a ranging metric in 3-D space, further antenna characterisation and modelling, along with relative attitude data provided by an IMU, may improve the range estimates by scaling the PLM function according to the relative attitude between two femto-spacecraft. This would be possible by explicitly considering the directivity of the antenna and

relating this to the attitude of the femto-spacecraft. It is also possible that the PCB material interferes with the radiation pattern, meaning that the propagation behind the antenna as implemented on the development kits (see Fig. 2) may be reduced, making this an additional effect to consider in 2-D space. This effect has been neglected for this experimental testing.

The PLM function was developed by taking all RSSI samples gathered at known (measured) ranges between nodes in the outdoor testing environment. The data used in the function is a combination of PLM-specific data and experimental positioning data. The distinction is that the specific PLM data was gathered at uniform ranges away from a single node, entirely for the purposes of developing a perfect case path loss model in the testing environment. The experimental positioning data comes from the many configurations of multiple tests used for demonstrating relative positioning and developing the experiment throughout the testing programme. No observable differences are shown in both sets of data (as expected). All testing was performed with a transmit power of 14 dBm.

The PLM was developed in MATLAB using the curve fitting toolbox. Logarithmic space was used for range to develop a simple linear model following the log-range model from Eq. 2. This results in a linear model with two coefficients that can be tuned as new modelling data is gathered. Experimental results of this modelling are given in Section 3.1.

2.3 Range-based Relative Positioning

In this section, we detail the algorithmic implementation of the ranging metric for experimental demonstration of range-based relative positioning and the testing environment used.

For the experimental demonstration we use the ranging metric data in two ways. Firstly, we apply a centralised localisation algorithm employing range-based semidefinite programming (SDP) from our previous simulation work [6]. This approach uses convex optimisation to localise femto-spacecraft as the centroids of feasible regions found by solving linear matrix inequalities (LMIs). In two-dimensional space, the objective is to find the $2 \times n$ matrix \mathbf{X} of unknown femto-spacecraft locations:

$$\mathbf{X} = \begin{bmatrix} x_1 & \cdots & x_n \\ y_1 & \cdots & y_n \end{bmatrix} \quad (3)$$

In summary, for a 2-D implementation, the algorithm finds the semidefinite matrix:

$$\mathbf{Z} = \begin{bmatrix} \mathbf{I}_2 & \mathbf{X}^T \\ \mathbf{X} & \mathbf{X}^T \mathbf{X} \end{bmatrix} \quad (4)$$

to minimise:

$$\sum_{(i,j) \in N_1} (\alpha_{ij}^+ + \alpha_{ij}^-) + \sum_{(k,j) \in N_2} (\alpha_{jk}^+ + \alpha_{jk}^-) \quad (5)$$

subject to:

$$\begin{pmatrix} e_{ij} \\ 0 \end{pmatrix}^T \mathbf{Z} \begin{pmatrix} e_{ij} \\ 0 \end{pmatrix} - \alpha_{ij}^+ + \alpha_{ij}^- = \hat{r}_{ij}^2 \quad \forall (i, j) \in N_1 \quad (6)$$

$$\begin{pmatrix} e_i \\ a_k \end{pmatrix}^T \mathbf{Z} \begin{pmatrix} e_i \\ a_k \end{pmatrix} - \alpha_{ik}^+ + \alpha_{ik}^- = \hat{r}_{ik}^2 \quad \forall (i, k) \in N_2 \quad (7)$$

where:

$$\mathbf{Z}, \alpha_{ij}^+, \alpha_{ij}^-, \alpha_{jk}^+, \alpha_{jk}^- \succcurlyeq 0 \quad (8)$$

and where $\alpha_{ij} = \alpha_{ij}^+ + \alpha_{ij}^-$ and $\alpha_{jk} = \alpha_{jk}^+ + \alpha_{jk}^-$ are the errors in the ranging measurements. \mathbf{I}_2 is a 2×2 identity matrix, e_{ij} is a zero column vector with the value of 1 at point i and the value of -1 at point j , and e_i is a zero column vector with the value of 1 at point i . The measured range between femto-spacecraft i and femto-spacecraft j is given by \hat{r}_{ij} , and \hat{r}_{jk} is the measured range between femto-spacecraft j and anchor k . Anchors are other spacecraft of known position. The set N_1 contains the pairs of femto-spacecraft (i, j) that have a range estimate \hat{r}_{ij} between them. The set N_2 contains the pairs of femto-spacecraft i and anchor k that have a range estimate \hat{r}_{ik} between them. Equation 8 indicates variables or matrices that are positive semidefinite. As the matrix \mathbf{Z} contains \mathbf{X} , the relative positions can be extracted from the solution.

Additionally, for single femto-spacecraft localisation, we use a method that was first shown in [9] of using normal probability density functions (NPDFs) of the range data for localisation. This method uses the confidence bounds of the PLM to create range annuli, where the intersections of annuli represent the highest likelihood of location from the coarse range estimates. This is effectively a form of 2-D trilateration. Both approaches work well to compensate for the inaccuracy of RSSI as a ranging metric by focusing on creating binding regions where a femto-spacecraft may lie within. Both algorithms are implemented in MATLAB.

The NPDF localisation method can be visualised as a heat map by summing these functions over a 2-D plane, resulting in a region of highest probability

emerging to localise the development kits relative to one another. The NPDFs take the form:

$$Z(x, y) = \frac{1}{\sqrt{2\pi\sigma^2}} e^{-\frac{(\sqrt{(x-a)^2+(y-b)^2}-\mu)^2}{2\sigma^2}} \quad (9)$$

where Z is the 3-D representation of probability, x and y are locations in 2-D space, a and b are 2-D coordinates of the transmitter, σ is the standard deviation in range (found from the path loss model), and μ is the mean of the range.

An aerial view of the testing region is shown in Fig. 5, showing a sports pitch at the University of Glasgow’s Garscube Sports Complex. This environment is ideal for this experiment as the area is wide, open and flat, and the length-scale used is representative of a swarm of femto-spacecraft in orbit. Development kits are placed approximately one metre off the ground on top of tripods made of bamboo to minimise interference. For the results shown in Sections 3.2 and 3.3, 13 development kits were placed in the testing area, 8 along the perimeter and 5 in the middle. An extra development kit connected to a laptop used for data logging operated close to but outside of the testing area.

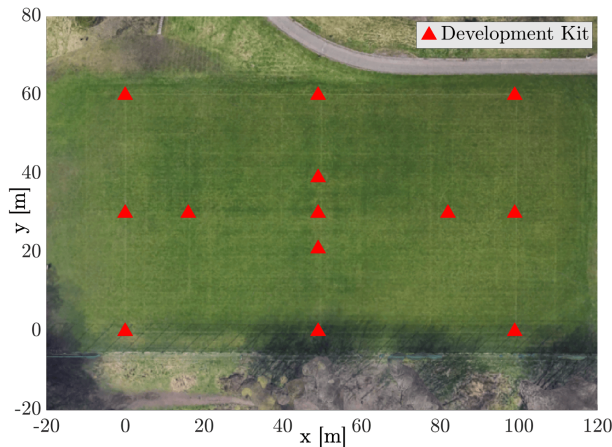


Fig. 5: Development kit placement in the testing environment. Imagery and map data credits: [10]

A series of relative positioning tests were performed by using some development kits as anchors, with their positions already known to the relative positioning algorithms. The algorithms are only provided with the RSSI data between anchors and unknown nodes to be localised, along with RSSI data shared between unknown nodes.

The implementation of relative localisation in space may not be able to rely on anchor nodes. It is possible that the realisation of this approach could

use multiple GPS-equipped carrier CubeSats as anchors. However, in the case of applications beyond low Earth orbit (LEO) and of single carrier CubeSats or other GPS-denied environments, it is necessary that the swarm is able to localise itself in relative space in the absence of anchors. For this, a method of relative frame initialisation would be required. This relative frame represents a coordinate system that all unknown femto-spacecraft are localised in. To do this, an algorithm to form anchors in a relative frame robust against uncertainties may be used, as detailed in our previous work [6]. Experimental testing of this method will be the subject of future work. Results given in Section 3 show the build up of using anchor nodes known to localise multiple femto-spacecraft of unknown location in 2-D.

3. Results and Discussion

3.1 Experimental derivation of the path loss model

The path loss model required to correlate RSSI to range was derived using all RSSI data gathered experimentally at measured distances as described in Section 2.2. The function derived using the MATLAB curve fitting tool for the testing environment (up to a distance of 140 m) is:

$$RSSI(r) = c_1 \log_{10}(r) - c_2 \quad (10)$$

and where the coefficients c_1 and c_2 are defined as (with 95% confidence bounds given in brackets):

$$c_1 = -22.91(-23.21, -22.61) \quad (11)$$

$$c_2 = -20.64(-21.17, -20.12) \quad (12)$$

Inverting this function, we obtain:

$$r(RSSI) = 10^{\left(\frac{RSSI-c_2}{c_1}\right)} \quad (13)$$

providing a function for a range estimate for a given RSSI value. This can then be used as an input for the relative positioning algorithms. The path loss model is shown in Fig. 6, showing all RSSI data used to generate the function, along with the 95% confidence bounds.

The distribution of RSSI data is noticeable, showing the inaccuracy of raw RSSI data as a range estimate, with considerably larger variation as range increases. Ultimately, as the confidence bounds in the model are accounted for with the algorithmic implementation, and as the number of femto-spacecraft in the swarm increases, the expected effect of fused data is to compensate considerably for this inaccuracy.

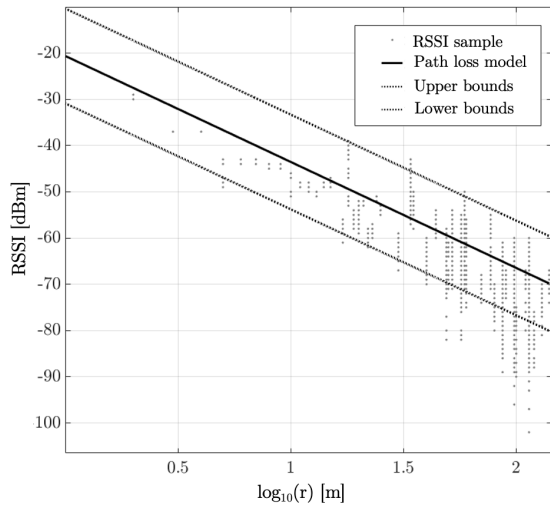


Fig. 6: Experimentally derived path loss model

3.2 Localisation of one femto-spacecraft

For a primary demonstration of relative localisation, the development kits were placed in the configuration shown in Fig. 5, with one development kit used as the unknown node to be localised. In this scenario, the 12 remaining development kits act as pre-localised anchors. This test was performed five times, once for each of the development kits located within the perimeter of the testing area. The objective of these tests is to establish if the anchors can localise the unknown development kit.

Figure 7 shows the localisation results for unknown node 1. Both the NPDF regions and the results of the SDP algorithm are shown. The 2-D coordinate estimates are taken from the centroids of both methods. The NPDF centroid error is 7.8 m, and the SDP centroid error is 21.4 m. Figure 8 shows the localisation results for unknown node 2. The NPDF centroid error is 20.4 m, and the SDP centroid error is 11.5 m. Figure 9 shows the localisation results for unknown node 3. The NPDF centroid error is 7.4 m, and the SDP centroid error is 4.7 m. Figure 10 shows the localisation results for unknown node 4. The NPDF centroid error is again 7.3 m, and the SDP centroid error is 1.3 m. Figure 11 shows the localisation results for unknown node 5. The NPDF centroid error is 7.0 m, and the SDP centroid error is 4.3 m.

This set of results demonstrate the ability of both methods to localise an unknown femto-spacecraft relative to many others. The solutions are comparable, with the SDP algorithm performing slightly better than the NPDF approach in most scenarios. It is anticipated that the accuracy of relative positioning

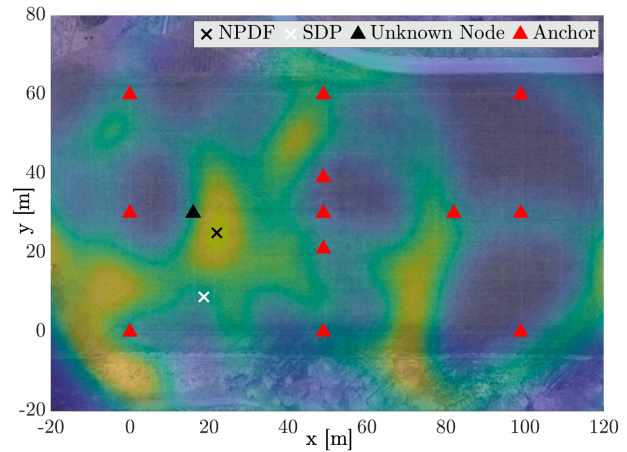


Fig. 7: Localisation of unknown node 1

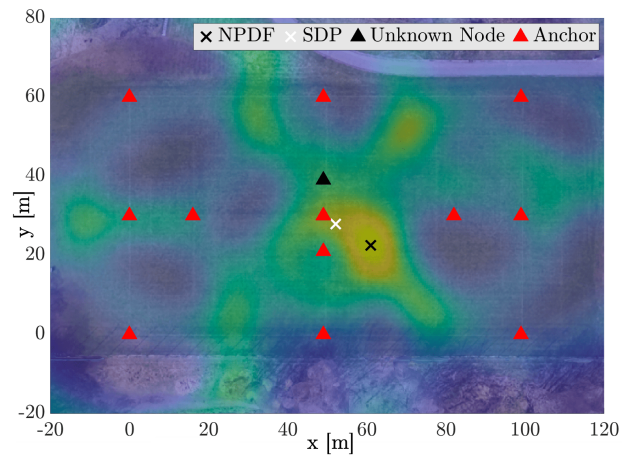


Fig. 8: Localisation of unknown node 2

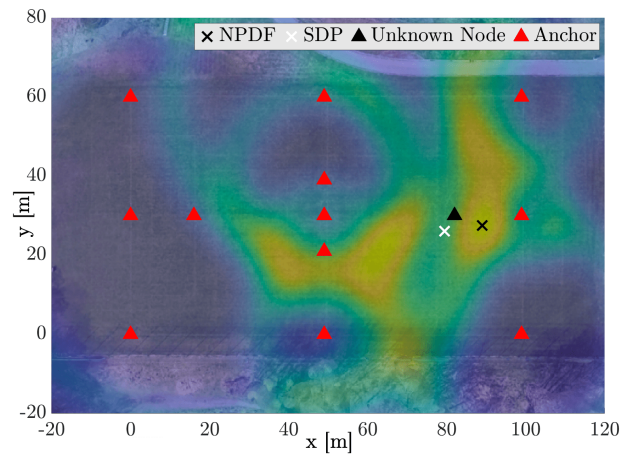


Fig. 9: Localisation of unknown node 3

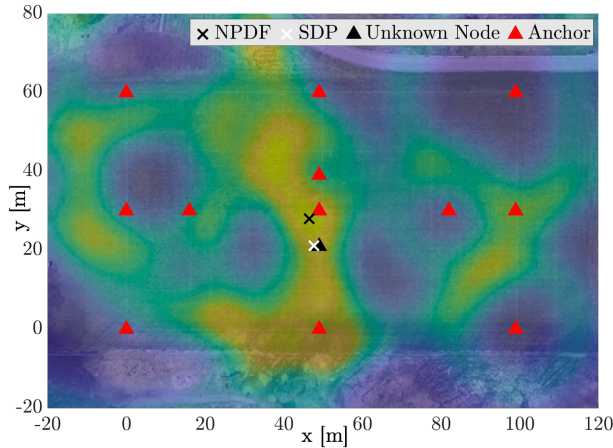


Fig. 10: Localisation of unknown node 4

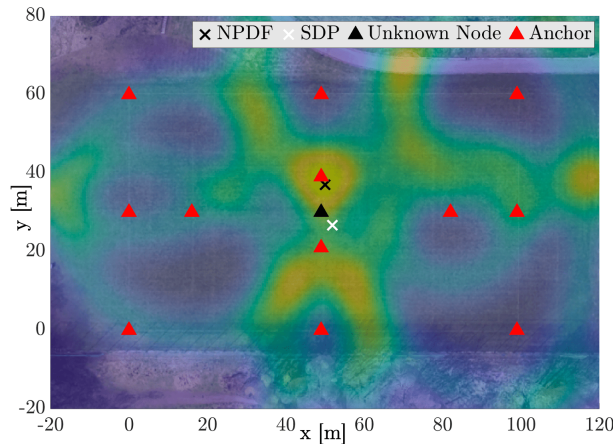


Fig. 11: Localisation of unknown node 5

will improve with larger scale tests in the future with more development kits, offering more insight into the expected performance levels in-orbit for a swarm.

3.3 Localisation of multiple femto-spacecraft

For swarm localisation it is necessary to localise many femto-spacecraft at the same time. Using the same configuration again, the 5 development kits localised individually using 12 anchors in Section 3.2 are now localised simultaneously, with only 8 anchors available along the perimeter of the testing area. The objective of this test is to establish if fewer anchors can localise multiple unknown development kit locations at once.

As there are fewer anchors, it would be expected that the NPDF method performs worse than in Section 3.2, owing to having 4 fewer range constraints to combine probabilities with. Conversely, with the

SDP algorithm able to now also utilise the RSSI data shared between the unknown nodes, it would be expected that the localisation performance is better than if the SDP algorithm were to localise only one node with 8 anchors.

Figure 12 shows the localisation results using SDP algorithms are shown. Equivalent single localisation estimates using the NPDF method are shown using 8 anchors for comparison. Range error lines are shown to each node to clarify which node the estimate is of, and the NPDF regions for each node are displayed to the right of the main results for each node. The 2-D coordinate estimates are again taken from the centroids of both methods. The mean SDP centroid error is 11.0 m and the mean NPDF centroid error is 20.1 m.

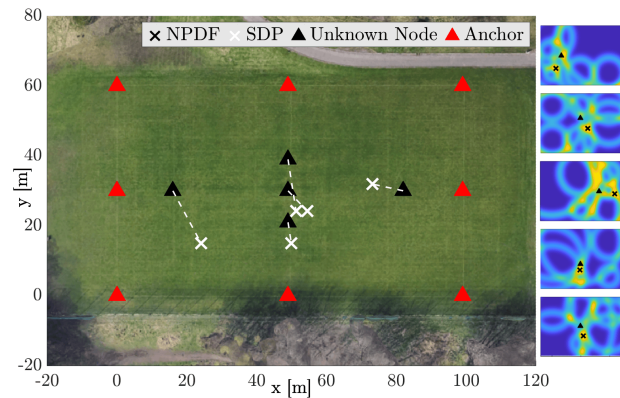


Fig. 12: Localisation of 5 unknown nodes

This demonstrates the ability of the SDP algorithm to localise multiple femto-spacecraft. As can be expected, the performance is lower than the single localisation case, but this could be improved with a larger number of devices in future tests and with relative frame localisation of anchors.

4. Conclusions

In this paper, the methodology and results of an experimental testing programme for the relative navigation of a swarm of femto-spacecraft have been presented.

A packet radio network protocol for the TI-CC1310 MCU has been developed and tested to work with full network interconnectivity enabling all RSSI data throughout the network to be regularly and reliably sampled. A path loss model was created to convert RSSI data into an approximation for a range measurement. This model was implemented to test

convex optimisation and probability-based methods for localisation.

The results demonstrate the viability of this method, through fusing coarse constraints to provide a relative positioning system for a swarm of femto-spacecraft entirely via networking. This would be invaluable to swarm applications in providing an estimate of where measurements are taken and when.

Future work will extend the experimental testing to three dimensions and dynamic femto-spacecraft. This will include one-to-one scaling of the relative dynamics to further expand the demonstration for future space applications, along with using larger networks to test distributed localisation algorithms for swarms.

Acknowledgements

This work was supported by the Royal Academy of Engineering under the Chair in Emerging Technologies scheme (Colin R McInnes). Thomas Timmons acknowledges the support of an EPSRC studentship (EP/R513222/1). The authors wish to thank Allan and all the ground staff team at the University of Glasgow's Garscube Sports Complex for all their assistance making the sports pitches available, and everyone who lent a hand setting up the experiments.

References

- [1] A. M. Hein, Z. Burkhardt, and T. M. Eubanks, "AttoSats: ChipSats, other Gram-Scale Spacecraft, and Beyond," in *Proceedings of the 70th International Astronautical Congress (IAC)*, (Washington D.C.), 2019.
- [2] F. Y. Hadaegh, S. J. Chung, and H. M. Manohara, "On Development of 100-gram-class spacecraft for swarm applications," *IEEE Systems Journal*, vol. 10, no. 2, pp. 673–684, 2016.
- [3] Z. R. Manchester and M. A. Peck, "Stochastic space exploration with microscale spacecraft," in *AIAA Guidance, Navigation, and Control Conference*, (Portland, Oregon), 2011.
- [4] T. Timmons, J. Beeley, G. Bailet, and C. R. McInnes, "Massively Parallel In-situ Sensing using Femto-spacecraft Clouds," in *Proceedings of the 72nd International Astronautical Congress (IAC), IAC-21-B4.7.4 (64209)*, (Dubai, United Arab Emirates), 2021.
- [5] H. Friis, "A Note on a Simple Transmission Formula," *Proceedings of the IRE and Waves and Electrons*, pp. 254–256, 1946.
- [6] T. Timmons, J. Beeley, G. Bailet, and C. R. McInnes, "Range-based Relative Navigation for a Swarm of Centimetre-scale Femto-spacecraft," *Journal of Guidance, Control, and Dynamics*, vol. 45, pp. 1583–1597, 2022. <https://arc.aiaa.org/doi/abs/10.2514/1.G00626>.
- [7] Texas Instruments, "TI LAUNCHXL-CC1310 Simplelink™Sub-1 GHz CC1310 wireless MCU LaunchPad™development kit," Available at <https://www.ti.com/tool/LAUNCHXL-CC1310>, last accessed August 2022.
- [8] Texas Instruments, "TI Easylink API rfEasyLinckEchoRx/rfEasyLinkEchoTx example project," Available at https://dev.ti.com/tirex/explore/node?node=AHEa3WR.QEVUptFfA3.G2A__eCfARaV__LATEST, last accessed August 2022.
- [9] T. Karlsson and M. Persson, "Outdoor localization in long range WSN using trilateration," 2017.
- [10] Imagery: ©2022 Google, Getmapping plc, Infoterra Ltd & Bluesky, Maxar Technologies, The GeoInformation Group. Map Data: ©2022 Google